European Journal of Pharmaceutical Sciences 150 (2020) 105335

Contents lists available at ScienceDirect

European Journal of Pharmaceutical Sciences

journal homepage: www.elsevier.com/locate/ejps

Carvacrol loaded nanostructured lipid carriers as a promising parenteral formulation for leishmaniasis treatment

Juliana G. Galvão[a], Raquel L. Santos[a], Audrey R.S.T. Silva[b], Jeferson S. Santos[a], Amanda M.B. Costa[a], Hardik Chandasana[c], Valter V. Andrade-Neto[d], Eduardo Caio Torres-Santos[d], Ana Amélia M. Lira[a], Silvio Dolabella[b], Ricardo Scher[b], Peter E. Kima[e], Hartmut Derendorf[c], Rogéria S. Nunes[a,*]

[a] Pharmacy Department, Federal University of Sergipe, Av. Marechal Rondon, s/n, Cidade Universitária, 49100-000 São Cristóvão, Sergipe, Brazil
[b] Morphology Department, Federal University of Sergipe, 49100-000 São Cristóvão, Sergipe, Brazil
[c] Department of Pharmaceutics, University of Florida, 32610 Gainesville, FL, United States
[d] Laboratório de Bioquímica de Tripanosomatídeos, Instituto Oswaldo Cruz, Fiocruz, Rio de Janeiro, Brazil
[e] Department of Microbiology and Cell Science, University of Florida, 32610 Gainesville, FL, United States

ARTICLE INFO

Keywords:
Solid lipids
Phenolic monoterpene
Natural products
Leishmania
Nanomedicine
Intravenous treatment

ABSTRACT

Leishmaniasis are a group of neglected infectious diseases caused by protozoa of the genus *Leishmania* with distinct presentations. The available leishmaniasis treatment options are either expensive and/or; cause adverse effects and some are ineffective for resistant *Leishmania* strains. Therefore, molecules derived from natural products as the monoterpene carvacrol, have attracted interest as promising anti-leishmania agents. However, the therapeutic use of carvacrol is limited due to its low aqueous solubility, rapid oxidation and volatilization. Thus, the development of nanostructured lipid carriers (NLCs) was proposed in the present study as a promising nanotechnology strategy to overcome these limitations and enable the use of carvacrol in leishmaniasis therapy. Carvacrol NLCs were obtained using a warm microemulsion method, and evaluated regarding the influence of lipid matrix and components concentration on the NLCs formation. NLCs were characterized by DSC and XRD as well. In addition, to the *in vitro* carvacrol release from NLCs, the *in vitro* cytotoxicity and leishmanicidal activity assays, and the *in vivo* pharmacokinetics evaluation of free and encapsulated carvacrol were performed. NLCs containing carvacrol were obtained successfully using a warm microemulsion dilution method. The NLCs formulation with the lowest particle size (98.42 ± 0.80 nm), narrowest size distribution (suitable for intravenous administration), and the highest encapsulation efficiency was produced by using beeswax as solid lipid (HLB = 9) and 5% of lipids and surfactant. The *in vitro* release of carvacrol from NLCs was fitted to the Korsmeyer and Peppas, and Weibull models, demonstrating that the release mechanism is probably the Fickian diffusion type. Moreover, carvacrol encapsulation in NLCs provided a lower cytotoxicity in comparison to free carvacrol ($p < 0.05$), increasing its *in vitro* leishmanicidal efficacy in the amastigote form. Finally, the *in vivo* pharmacokinetics of carvacrol after IV bolus administration suggests that this phenolic monoterpene undergoes enterohepatic circulation and therefore presented a long half-life ($t_{1/2}$) and low clearance (Cl). In addition, C_0, mean residence time (MRT) and V_{dss} of encapsulated carvacrol were higher than free carvacrol ($p < 0.05$), favoring a higher distribution of carvacrol in the target tissues. Thus, it is possible to conclude that the developed NLCs are a promising delivery system for leishmaniasis treatment.

1. Introduction

Neglected Tropical Diseases (NTDs) comprises several infectious diseases predominant in the poorest regions of the world. These diseases are prevalent in tropical and sub-tropical areas, due to insufficient sanitary conditions. It is estimated that currently there are approximately 20 NTDs prevalent in 149 countries, affecting one billion people worldwide. Among NTDs, it is estimated that annually around 700.000 to 1 million new cases of leishmaniasis occur and 20.000 to 30.000 of deaths worldwide (de Souza et al., 2018; World Health Organization (WHO)., 2018).

Leishmaniasis is caused by protozoa of the genus *Leishmania* in the

* Corresponding author.
E-mail address: rogeria.ufs@hotmail.com (R.S. Nunes).

https://doi.org/10.1016/j.ejps.2020.105335
Received 15 October 2019; Received in revised form 11 March 2020; Accepted 30 March 2020
Available online 06 April 2020
0928-0987/

family Trypanosomatidae. This disease presents in two main forms, cutaneous leishmaniasis (CL) and visceral leishmaniasis (VL) (Tiuman et al., 2011). According to the World Health Organization, 25 countries were considered high burden for leishmaniasis in 2015, which means they present over 100 cases of VL and over 2500 of CL. Among these countries, Brazil is the only country to present high burden for both forms of leishmaniasis (de Souza et al., 2018; Organization, 2016). In Brazil, there were 3200 registered cases of VL and 12,690 cases of CL, with the Northeast region most affected by VL with 1523 (47.59%) cases and North region most affected by CL with 5075 (39.99%) registered cases (Ministério da saúde, 2017; Saúde, 2017).

Thus, from an epidemiological point of view leishmaniasis can be considered a public health issue and a major concern for the health surveillance agencies. Since the control of insect vector is difficult and no effective vaccine exists, chemotherapy is the main means of dealing with this disease. In the past 70 years, pentavalent antimonials - sodium stibogluconate (Pentostam®) and meglumine antimoniate (Glucantime®) -, amphotericin B, pentamidine, paromomycin and miltefosine have been used as gold standard treatment of leishmaniasis (Pham et al., 2014, 2013; Tiuman et al., 2011).

However, conventional leishmaniasis treatment options may cause some undesirable adverse effects such as gastrointestinal disorders, kidney and liver toxicity (Pham et al., 2013). In addition, some of these drugs are expensive, *Leishmania* species from different strains have shown different susceptibility to them, and resistance of some isolates and/or strains to some drugs have been reported, especially, with antimonials and miltefosine. Thus, there is an urgent need for new molecules to treat *Leishmania* infections (de Medeiros et al., 2011; Pastor et al., 2015).

Besides the synthesis of drugs, the research of natural products may provide new promising molecules. Nowadays, medicinal plants and/or several of its derivative compounds are employed in the treatment of diseases. As examples, paclitaxel and vinca alkaloids are used in cancer treatment, while artemisinin is a potent molecule against malaria (Polonio and Efferth, 2008).

Carvacrol (CRV) is a phenolic monoterpene that presents various pharmacological activities such as analgesic (de Sousa, 2011), anti-inflammatory (Silva et al., 2012), antimicrobial (Belda-Galbis et al., 2014), antitumoral (Arunasree, 2010), antioxidant (Beena et al., 2013) and anti-leishmania (Monzote et al., 2014). It is believed that because of its hydrophobic nature, carvacrol is able to be preferentially incorporated in the cell membrane, which renders them permeable to protons and ions as well as affecting vital enzymatic function of the microorganisms (de Medeiros et al., 2011). Furthermore, Silva et al. (2017) observed that the presence of the hydroxyl group associated with the benzene ring in the carvacrol molecule plays an important role for anti-leishmania activity.

De Melo et al. (2013) reported the anti-leishmania activity of carvacrol, which demonstrated lethal inhibition concentration to 50 percent of the *Leishmania chagasi* (IC_{50}) of 2.3 μg mL^{-1}. In L. *amazonensis* strains, Pastor et al. (2015) and Monzote et al., 2014 observed for carvacrol IC_{50} of 15.3 ± 4.6 ug.mL^{-1}. Moreover, *in vivo* studies in mice demonstrated a reduction in lesion size, caused by cutaneous leishmaniasis, after intralesional administration of 30 mg/kg of carvacrol once a day for 15 days in comparison to control group (Monzote et al., 2014).

Nevertheless, carvacrol exhibits low aqueous solubility, due to its lipophilic nature, rapid oxidation and volatilization, limiting its therapeutic application (Santos et al., 2015). The encapsulation of hydrophobic compounds, such as carvacrol, in colloidal carriers is a possible strategy to overcome these limitations (Bruni et al., 2017; De Almeida et al., 2017). Furthermore, nanoparticles ranging in size from 50 to 500 nm especially, have the advantage of being easily internalized by macrophages that are the main phagocytic cells that hosts *Leishmania* parasites. Internalization of nanoparticles by macrophages may increase intracellular drug concentration, specifically in the parasitic vacuole, where *Leishmania* reside (Bruni et al., 2017). This mechanism might favor the increase of therapeutic efficacy by release of active compound directly in macrophage-rich organs such as bone marrow, liver and spleen (de Souza et al., 2018).

Nano-sized carriers such as lipid nanoparticles have been reported to improve the efficacy of the known anti-leishmania and anti-malaria agents, amphotericin B and oryzalin, respectively (Lopes et al., 2012). Nanostructured Lipid Carriers (NLCs) consist in nanometric particles obtained from mixtures between solid and liquid lipids dispersed in a surfactant solution, remaining solids at room and corporal temperature (Müller et al., 2007). Due to its nanoparticulate and matrix nature, NLCs have some advantages such as the controlled release of substances, due to the solid state of the lipid matrix, the improvement of drug stability, low toxicity and biocompatibility, being promising release systems for parenteral or non-parenteral administration of molecules for leishmaniasis treatment (Guterres et al., 2007; Mehnert and Mäder, 2012; Müller et al., 2000).

Thus, the aim of this work was to encapsulate CRV in a pharmaceutically acceptable formulation of NLCs for parenteral administration. This study assesses the influence of manufacturing parameters, such as the choice of solid lipid, surfactant and lipid concentration, as well as the stability during storage time. In addition, the *in vitro* carvacrol release from NLCs, the *in vitro* cytotoxicity and leishmanicidal activity assays, and the *in vivo* pharmacokinetics evaluation of free carvacrol and encapsulated were accessed as well.

2. Material

Stearic acid (SA) was purchased from Dinâmica® and beeswax (BW) from GM Ceras (São Paulo, SP, Brazil). Carvacrol (≥ 99%), *p*-cresol (≥99.5%) and Kolliphor188® were acquired by Sigma Aldrich® (St. Louis, MO, USA). Acetonitrile (ACN) and acetic acid HPLC grade were obtained from Fisher Scientific® (Fairlawn, NJ). Drug-free Wistar rat plasma with sodium heparin was purchased from Innovative Research, Inc., (Novi, MI). All the other solvents were acquired from Fisher Scientific®.

3. Methods

3.1. Preparation of NLCs by warm microemulsion method

NLCs were prepared by warm microemulsion oil in water (O/W) adapted from Souza et al. (2011). Firstly, the oily phase containing a mixture of the solid lipid (SA or BW) and carvacrol as liquid lipid in 7:3 ratio was heated up to 10 °C over the solid lipid melting point. The aqueous phase composed of the surfactant Kolliphor 188® (known as poloxamer 188) was dispersed in ultrapure water and heated up to approximately to the same temperature of the oily phase. Then, the aqueous phase was poured into the oily phase and submitted to an ultrasom Sonics (Newtown, EUA) Vibracell® 130 W model at 50% of amplitude for 10 min. Finally, the coarse emulsion was immediately dispersed in cold water at 2 to 4 °C (placed in an iced bath) in 1:10 ratio followed by stirring at 3400 rpm for 3 min in Ultra-turrax IKA® (Staufen, Germany) T25 model.

For DSC and XRD analysis the resultant nanodispersion was freeze-dried by Freeze Dryer LS3000 TERRONI® for 48 h.

3.2. Factorial design

For the evaluation of the lipid matrix influence on the hydrodynamic radius, polydispersity index (PdI) and zeta potential of the free and carvacrol loaded NLCs, a 2^2 factorial design was performed. The variables analyzed were the hydrophilic-lipophilic balance (HLB) required by the solid lipids (9 for BW and 15 for SA) and the lipids (solid + liquid lipids) concentration in the coarse emulsion (2 and 5% w/v). In this case, the surfactant concentration was kept constant at 1%

in all obtained formulations.

A second factorial design 2^2 was performed aiming the evaluation of the lipids (2 and 5% w/v) and surfactant concentration (1 and 5% w/v) on the hydrodynamic radius, polydispersity index (PdI), zeta potential, encapsulation efficiency (EE%) of the free and carvacrol loaded NLCs. In this case, the solid lipid used was the BW.

The NLCs formulations were developed following these factorial designs and the obtained results were submitted to STATISTICA® 10.0 (StatSoft Inc®, Tulsa- US) software. The analysis of variance (ANOVA) of the influence of variables and their interactions were performed, being $p < 0.05$ values considered statistically significant.

3.3. HPLC quantification method of carvacrol

All analyses were performed on YL9100 HPLC System (Anyang-si, Korea) equipped with a PDA detector (Model YL9160) operating at 274 nm, a quaternary pump (Model YL9110), a vacuum degasser (Model YL9101), an autosampler (Model YL9150) and a column oven (Model YL9130) at the temperature of 35 °C. A Agilent® Zorbax C18 column (150 × 4.6 mm, 5 μm packing, Santa Clara, EUA) was used. The mobile phase consisted of acetonitrile: water acidified with acetic acid 1% (60:40) at a flow rate of 1 mL min^{-1}. The methodology was validated to ensure the reliability of results. All measurements were performed in triplicate.

3.4. Characterization of NLCs

3.4.1. Particle size, polidispersity index and zeta potential

The particle size, polydispersity index (PdI) and Zeta potential of the prepared NLCs were determined by dynamic light scattering (DLS) using a Zetasizer Nano ZS (Malvern Instruments®, UK) with a fixed detector at an angle of 173°, and a 35 mW He-Ne laser with wavelength of 633 nm, at 25 °C. Whenever needed, the samples were diluted with ultrapure water to an appropriate concentration, prior to measurement in order to prevent multiscattering effects. Zeta potential was obtained by the conversion of electrophoretic mobility according to the method of Helmholtz-von Smoluchowski. All measurements were carried out in triplicate.

3.4.2. Encapsulation efficiency (EE%)

The encapsulation efficiency of carvacrol in the NLCs was determined by the indirect method described by Ribeiro et al. (2016). The NLCs containing carvacrol were centrifuged in a Eppendorf 5804R model (Hamburg, DE) centrifuge using Vivaspin 500 Sartorius® (Göttingen, DE) tubes, equipped with ultrafilters of 10.000 MWCO, at 14.000 rpm for 30 min at room temperature. Afterwards, the amount of "free" carvacrol present in the filtered part was quantified by a HPLC quantification method previously validated. The EE% of carvacrol in the NLCs was calculated by the following Eq. (1):

$$EE\% = \frac{(\text{CRV used in NLC preparation}) - (\text{CRV filtered})}{(\text{CRV used in NLC preparation})} \times 100 \quad (1)$$

To perform the next characterizations, *in vitro* release experiments, *in vitro* cytotoxicity, *in vitro* leishmanicidal activity and *in vivo* pharmacokinetics a CRV-NLCs formulation with 5% (w/v) of lipids, 5% (w/v) of surfactants and 1500 μg/mL of carvacrol was chosen.

3.4.3. Differential scanning calorimetry

DSC curves were obtained by DSC NETZSCH DSC 200 F3 (Selb, Germany). The solid lipid beeswax, poloxamer 188, and freeze-dried free and carvacrol loaded NLCs (3 to 5 mg) were placed in aluminum crucibles and analyzed in the temperature range of 25 to 300 °C, heating rate of 10 °C min^{-1}, and nitrogen dynamic atmosphere (50 mL min^{-1}).

3.4.4. X-ray diffraction

XRD analysis was performed in a Bruker (Billerica, USA) model D8 Advance; Radiation: Cu Kα (λ = 1594 Å). The solid lipid beeswax, poloxamer 188, and freeze-dried carvacrol loaded NLCs were analyzed in the range of 2 to 40° (2θ), speed of 1° min − 1, 40 kV and 40 mA.

3.4.5. Transmission electron microscopy (TEM and cryo-tem)

CRV-NLCs were deposited on ultrathin lacey copper grids and negatively stained with 2% (w/v) uranyl acetate and observed through a transmission electron microscope JEOL (Akishima, JP) JEM-1400Plus model at 120 kV. CRV-NLCs were also prepared for Cryo-TEM by quench-freezing thin liquid films in liquefied ethane. The vitrified specimen was transferred to the microscope for imaging on a liquid-nitrogen-cooled Gatan 626 cryoholder. The temperature of the sample was kept below −180 °C throughout the examination by using a transmission electron microscope JEOL (Akishima, JP) JEM-1400Plus model at 120 kV. A low-dose procedure was used to reduce radiation damage in the areas of interest.

3.4.6. In vitro release experiments

The *in vitro* release experiments were performed according the dialysis bag method reported by Fangueiro et al. (2016) adapted. Firstly, cellulose acetate 10.000 MWCO membranes Fisher Scientific® (Whaltam, EUA) were prepared as the supplier recommended. The release medium was composed of a mixture of phosphate buffer saline (pH 7.4) and ethanol in 7:3 ratio (v/v). A carvacrol solution (CRV-free) was prepared using the release medium. Afterwards, 2 mL of the carvacrol loaded NLCs (CRV-NLCs) that was selected in the previous experiments, and CRV-free were put in the dialysis bags and placed into a container containing 10 mL of the release medium. The system was kept at 37.0 ± 0.5 °C under magnetic stirring at approximately 30 rpm for 24 h. 300 μL of the release medium was collected after 0.25, 0.5, 1, 2, 3, 4, 5, 6, 8, 12 e 24 h of the experiment has started, being replaced by new release medium in order to maintain the sink conditions. The experiment was performed in sextuplicate.

The collected samples were quantified by a HPLC-UV quantification method previously validated. Carvacrol release data were analyzed by release kinetic models, including, zero order, first order, Korsmeyer & Peppas and Weibull models by the KinetDS Copyright (C) 2010 Aleksander Mendyk software (Sizílio et al., 2018).

3.4.7. In vitro cytotoxicity in differentiated human monocytic cell line

Human monocytic cells-line THP-1 (ATCC) were cultivated in RPMI 1640 medium with L-glutamine and 25 mM of HEPES at 37 °C and 5% of CO_2. For the differentiation to adherent macrophages, the culture was adjusted to a density of 5 × 10^6 cells/mL and 100 ng/mL of phorbol myristate acetate (PMA) were added. Then, 5 × 10^5 cells were seeded in each well of a 96 well plate and were incubated at 37 °C and 5% of CO_2 for 48 h. After the differentiation, the cells were washed and were incubated in RPMI medium, PMA free. After 24 h, differentiated THP-1 cells were incubated with different concentrations of carvacrol, CRV-NLCs (24.9–150 μg/mL) and a standard drug miltefosine (3–48.9 μg/mL) in RPMI medium at 37 °C and 5% of CO_2 for 48 h. Cells without treatment were used as negative control.

After the incubation time, the cells were exposed to 10 μL of MTT (Biotium kit) at 37 °C for 4 h. MTT is converted, from the viable cells, to formazan, and therefore, 200 μL of dimethyl sulfoxide (DMSO) were added in each well in order to solubilize formazan. The absorbance was measured by using a microplate reader at 570 nm and used to calculate the cell viability (%), according to the Eq. (2):

$$\text{Cell viability}(\%) = \frac{\text{Abs (treatment)} - \text{Abs (DMSO)}}{\text{Abs (negative control)} - \text{Abs (DMSO)}} \times 100 \quad (2)$$

The cytotoxic concentrations lethal to 50% of the cells (CC_{50}) were obtained by nonlinear regression of the sigmoid growth curves using the software Graph Pad Prism 5.0. The results were compared and

analyzed through the Student`s *t*-test, considering $p < 0.05$ as statistically significant.

3.4.8. In vitro promastigote activity

Promastigotes of L. *amazonensis* strain RAT/BA/74/LV78 originally provided by dr. Lynn Soong (UTMB, Texas) were maintained in Schneider medium (Sigma, St. Louis, MO, EUA) supplemented with 10% of heat-inactivated fetal bovine serum and 10 μg/mL gentamycin (Sigma, St. Louis, MO, EUA) at 24 °C. The parasite growth curve was obtained from the daily count of the culture for 7 days. Promastigotes in exponential growth phase (6–8 × 10^6 promastigotes/mL) were used for viability assay. The promastigotes were incubated with different concentrations of carvacrol, CRV-NLCs (6.25–100 μg/mL) and miltefosine (3 – 48.9 μg/mL) (positive control) in Schneider medium at 24 °C for 48 h. As negative control, the promastigotes were kept without any treatment.

After the incubation time, 10 μL of resazurin (TOX-8 *In vitro Toxicology Assay Kit Resazurin Based*, Sigma) were added in each well and the plate was incubated at 24 °C for 2 to 3 h. The absorbance was measured by using a microplate reader at 570 and 600 nm and used to calculate the promastigote viability (%), according to the Eq. (3):

$$\%\,\text{Viability} = \frac{(\text{Abs}\,570\,\text{nm} - (\text{Abs}\ 600\text{nm x RO})\text{test})}{(\text{Abs}\,570\,\text{nm} - (\text{Abs}\ 600\text{nm x RO})\text{control})} \times 100 \quad (3)$$

The inhibitory concentrations to 50% of the promastigotes (IC_{50}) were obtained by nonlinear regression of the sigmoid growth curves using the software Graph Pad Prism 5.0. The results were compared and analyzed through the Student`s *t*-test, considering $p < 0.05$ as statistically significant.

3.5. Antiamastigote activity

3.5.1. Maintenance and cultivation of parasites for antiamastigote activity

Leishmania amazonensis promastigotes (strain MHOM/BR/77/LTB 0016) were maintained at 26 °C in Schneider® medium (Sigma-Aldrich Corp., St. Louis, MO, USA) supplemented with 10% fetal bovine serum (FBS), 100 μg/mL streptomycin, 100 U/mL penicillin. Subcultures were performed twice a week until the 5th passage. The parasites were obtained from infected BALB/c mice.

3.5.2. Cytotoxicity to murine peritoneal macrophages

Murine peritoneal macrophages in 96-well plates were treated with carvacrol, lipid formulation at concentrations 7.5 - 960 μg/mL and amphotericin B (0.125 – 20 μg/mL) for 72 h at 37 °C/5%CO_2. After 72 h, resazurin sodium salt (500 μM) (Sigma-Aldrich Corp., St. Louis, MO, USA) was added to the macrophage cultures to a final concentration of 50 μM, and the plates were then incubated at 37 °C/5%CO_2 for additional 4 h. The fluorescence was measured at excitation/emission of 560/590 nm in Spectra Max GEMINI XPS (Molecular Devices, Silicon Valley, EUA). The number of viable treated macrophages was expressed as a percentage of the number of viable untreated-control macrophages (taken as 100%). Each point was tested in triplicate with three biological replicates.

3.5.3. In vitro antiamastigote activity assay

Peritoneal macrophages from BALB/c mice were infected with L. *amazonensis* promastigotes (stationary-growth phase) at a 3:1 parasite-to-macrophage ratio, incubated for 4 h in Lab-Tek chambers (Nunc, Roskilde, Denmark), and kept at 37 °C5%CO_2. After 24 h, the chambers were washed, and the cultures were treated with carvacrol, lipid formulation at concentrations 7.5 - 240 μg/mL and amphotericin B (0.04375 – 1.4 μg/mL) in RPMI medium supplemented with 10% FBS, 1% pyruvate and 1% glutamine for 72 h at 37 °C 5% CO_2. After incubation, the slides were stained, and the infection rate was determined by counting under a light microscope. The infection rate was calculated using the formula: (% of infected macrophages × average number of amastigotes per total number of macrophage). The 50% inhibitory concentration (IC_{50}), *i.e.*, the minimum drug concentration that caused a 50% reduction in infection rate in comparison with that in control infection without the compound, was obtained by non-linear regression using GraphPad Prism software. Each point was tested in duplicate with three biological replicates.

3.5.4. Animals

Healthy male cannulated in the jugular vein Wistar rats (weight 300 to 350 g) were obtained from Charles River Laboratories. The rats were fed with standard food pellets and maintained under standard laboratory conditions with a dark/light cycle of 12 h. All rats were fasted overnight before the experiments, but allowed access to water *ad libitum*. This study was previously approved by the local ethics committee "Institutional Animal Care and Use Committee" da *University of Florida* (Gainesville, FL) under the protocol number #201710000. The protocol was performed according to the *"Principles of Laboratory Animal Care"* (publication NIH #85–23, revised 1985).

3.5.5. In vivo pharmacokinetics study

The pharmacokinetic profile of CRV in rat plasma was determined through in bolus intravenous administration of 3 mg/kg of free carvacrol prepared in DMSO-saline solution for injection (CRV-S) and encapsulated (CRV-NLCs).

In the day of the experiment, 3 mg/kg of CRV-S and CRV-NLCs were administered in the lateral tail vein of 3 Wistar male rats (for each group) as a bolus. Nine blood samples (300 μL) were withdrawn from the cannula in the jugular vein and stored in EDTA-containing tubes after 0.17, 0.5, 1, 2, 4, 6, 8, 10 and 24 h after dosing. Each of the blood samples were centrifuged at 10.000 rpm for 10 min. Plasma sample analysis was performed using validated HPLC method (paper in communication). The plasma was immediately separated and stored at −80 °C until analysis. The resulting plasma (100 μL) was vortex-mixed with 900 μL of internal standard (*p*-cresol) in acetonitrile (3000 ng/mL) for 3 min and centrifuged at 12.000 rpm for 20 min. The supernatant (750 μL) was dried, reconstituted in 100 μL ACN and injected for HPLC analysis.

Non-compartmental analysis of the data was performed in Phoenix 8.0 software (Certara, Princeton, NJ). All pharmacokinetic parameters were calculated for each animal and, the average and standard deviation (SD) of each parameter were determined. The terminal elimination rate constant (λ_z) was estimated from the slope of terminal exponential phase of the logarithmic plasma concentration-time profile using at least 4 data points. Terminal elimination half-life ($t_{1/2}$) was calculated as $\ln(2)/\lambda_z$. The area under the concentration-time curve was calculated using the log-linear trapezoidal rule. Clearance (CL) was calculated as the dose divided by the $AUC_{0-\infty}$. The volume of distribution V_{dss} was calculated as the CL divided by λ_z. The mean residence time (MRT) was calculated as the area under the first moment curve ($AUMC_{0-\infty}$)/$AUC_{0-\infty}$.

4. Results and discussion

4.1. Influence of the lipid matrix on NLCs formation

Solid lipids play an important role on NLCs matrix composition and, consequently, small differences in its characteristics and properties, may lead to significant changes in NLCs formulations (Mitri et al., 2011; Müller et al., 2002; Yan et al., 2010). Teeranachaideekul et al. (2017) observed that in NLCs preparation, the adequate selection of lipid components has a great impact on the particle size, zeta potential, encapsulation efficiency, release profile, which may influence on NLCs features.

The influence of lipid matrix on particle size, polydispersity index, zeta potential of carvacrol loaded NLCs (CRV-NLCs) is shown in Fig. 1. Two solid lipids BW and SA with hydrophilic-lipophilic balance (HLB)

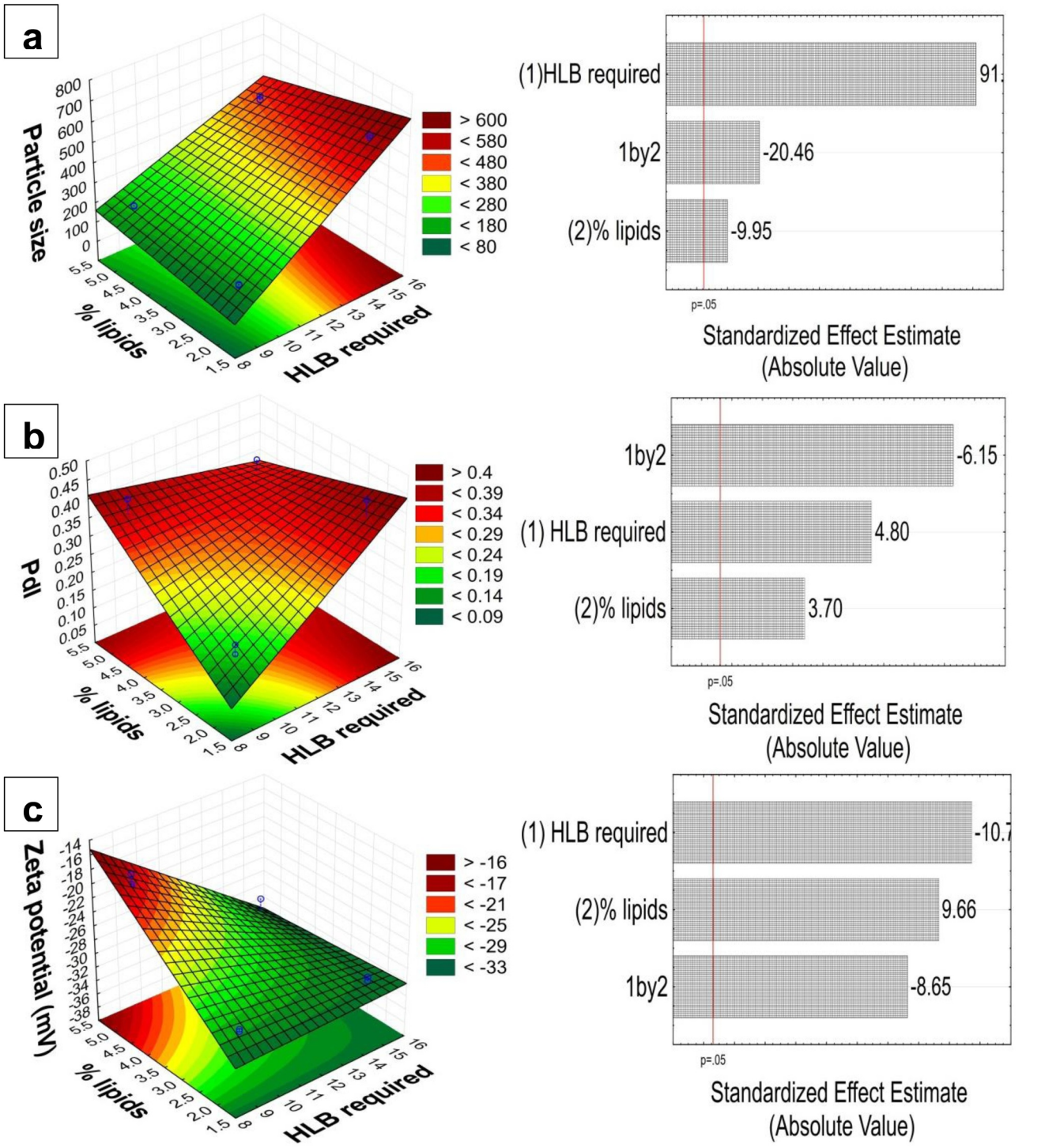

Fig. 1. Surface response charts of experimental design and pareto charts of the standardized effects for CRV-NLCs (a) particle size; (b) polydispersity index; (c) zeta potential in function of the% of lipids and the HLB required by the solid lipid. Color codes stand for the area below the given value. These results were obtained from STATISTICA® 10.0 software and were submitted to ANOVA statistical test, being $p < 0.05$ values considered statistically significant.

required of 9 and 15 respectively were tested in order to select the solid lipid best suited to NLCs formulation. In addition, two pre-emulsion lipid concentration were tested, 2% e 5% (w/v), keeping constant the surfactant concentration in 1%.

Regarding the particle size, we observed that the lower the HLB required by the solid lipid and its concentration (2%) the lower was the particle size (153 ± 2.90 nm). All NLCs formulations presented a narrow particle size distribution with PDI ≤ 0.5, being the CRV-NLCs prepared with BW and 2% of lipids, the formulation with the lowest PDI (0.166 ± 0.04), following the same trend of particle size results (Lakshmi and Kumar, 2010).

Another parameter evaluated was the zeta potential. Zeta potential (ξ) can be used to estimate the nanoparticles charge and/or its electrostatic repulsion. According to DLVO's theory the system will be considered stable, if the electrostatic repulsion dominates the Van der Walls attractive forces. In general, the aggregation of particles tends to occur less when the system presents high values of ξ ($> |30|$ mV), due to electrostatic repulsion (Han et al., 2008). In Fig. 1, we observed that all

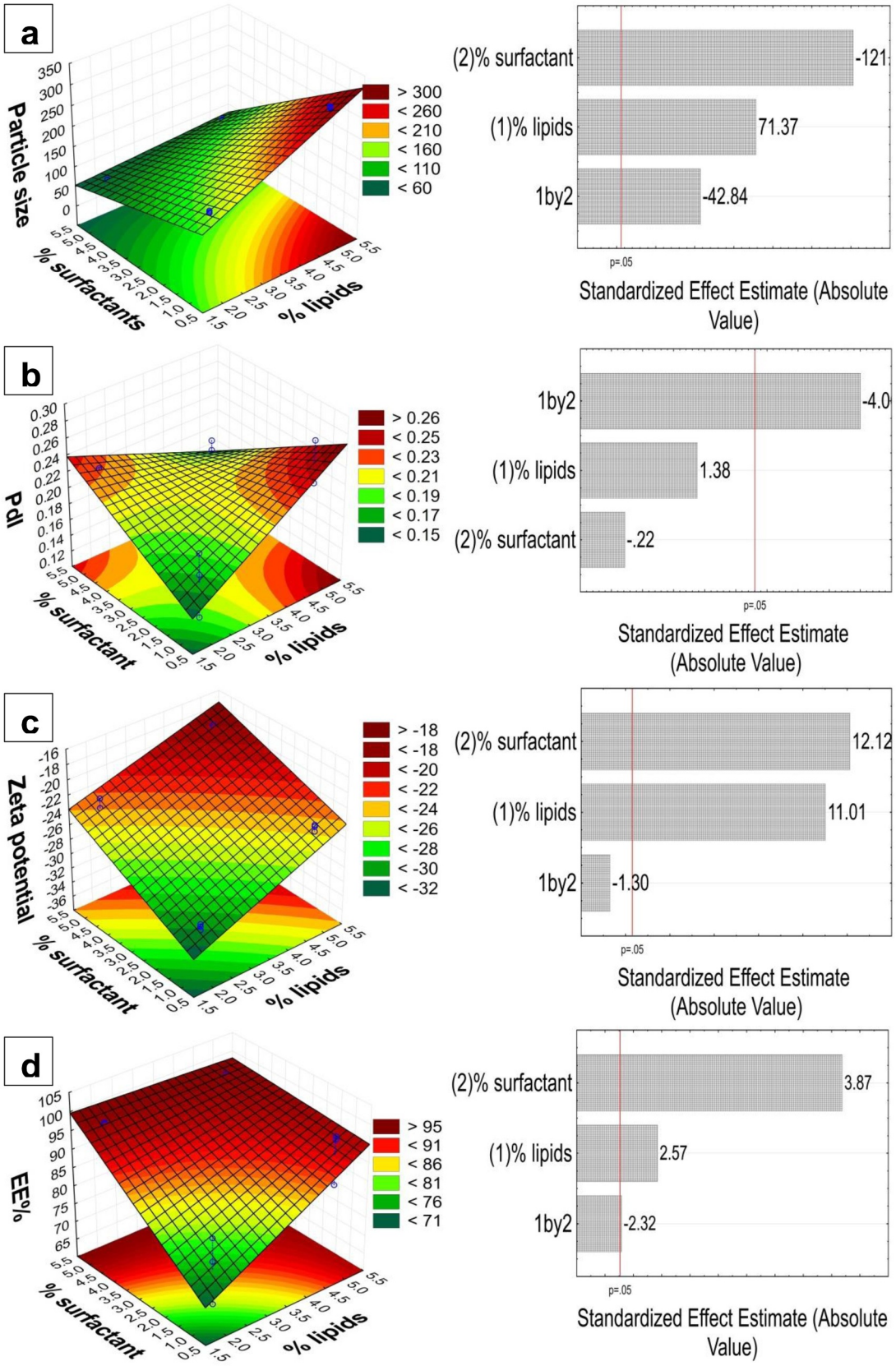

Fig. 2. Surface response charts of experimental design and pareto charts of the standardized effects for CRV-NLCs (a) particle size; (b) polydispersity index; (c) zeta potential; (d) encapsulation efficiency in function of the% of lipids and the% of surfactants. Color codes stand for the area below the given value. These results were obtained from STATISTICA® 10.0 software and were submitted to ANOVA statistical test, being $p < 0.05$ values considered statistically significant.

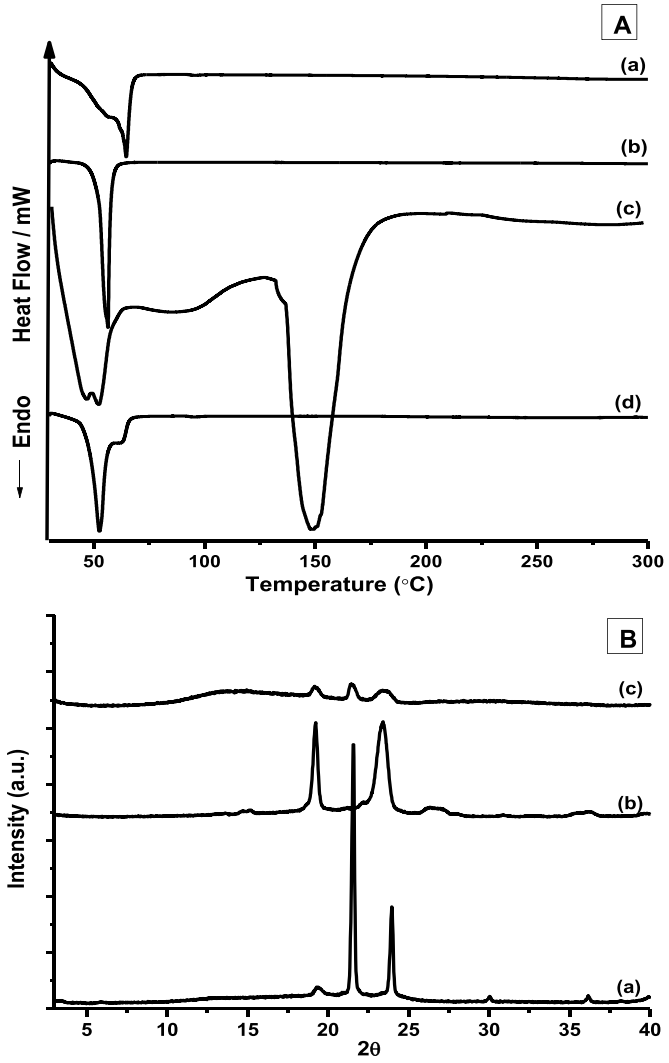

Fig. 3. A. DSC curves of the solid lipid beeswax (a), poloxamer 188 (b), physical mixture 1:1 (c) and CRV-NLCs (d). **B.** X-ray diffraction profile of the solid lipid beeswax (a), poloxamer 188 (b), and CRV-NLCs (c). The DSC curves were obtained with a heating rate of 10 °C min^{-1} and nitrogen dynamic atmosphere (50 mL min^{-1}).

NLCs formulations presented zeta potential between −20 and −30 mV. This result is expected for colloidal systems using non-ionic surfactants like poloxamer 188, since the main stabilization mechanism of these surfactants are due to steric repulsion, besides the electrostatic repulsion mechanism (Tsai et al., 2012).

As shown in Pareto charts of the standardized effects (Fig. 1), both studied variables and the interaction between them demonstrated statistically significant effect ($p < 0.05$) on particle size, PDI and zeta potential. In view of the presented results, the solid lipid (HLB = 9) was selected to prepare CRV-NLCs for enabling the formation of particles with the lowest size and narrowest size distribution.

Influence of lipid and surfactant concentration on NLCs formation and encapsulation efficiency of carvacrol

After the selection of the suitable solid lipid to NLCs formulation, the influence of lipid and surfactant concentration on particle size, PDI and zeta potential were evaluated. In Fig. 2, we observed that the lowest particle sizes were found for NLCs with the highest surfactant concentration (5%) and lowest lipid concentration (2%) tested. The p-value for both analyzed variables and its interaction showed statistically significant effect on particle size (Fig. 2). It is expected that NLCs formulations with higher surfactant concentration would present lower particle size due to a higher reduction of superficial tension in the system, favoring the interfacial film formation.

The opposite was observed when higher lipid concentration led to higher particle sizes. This was also reported by Schubert and Muller-Goymann (2003) (Schubert and Müller-Goymann, 2003) when evaluating the influence of lipid concentration on lipid nanoparticle characteristics, observed a significant increase on particle size by raising lipid concentration. Similarly, Yan et al. (2010) observed the same behavior and attributed the increase in particle size to the growth of pre-emulsion viscosity which consequently hamper the lipid emulsification in the aqueous phase, reducing the molecules diffusion rate in the external phase.

Regarding PDI, all NLCs formulations presented a narrow size distribution PdI ≤ 0.2, therefore being suitable to parenteral administration (Lopes et al., 2012). In this case, the variables have not demonstrated significant statistical impact on PDI, only the interaction between variables. In Fig. 2, we also observed that all NLCs formulations presented zeta potential between −20 and −30 mV, therefore being stable. The variables tested presented significant statistical effect on zeta potential, but not the interaction between them.

The influence of lipid and surfactant concentration on EE% of carvacrol was evaluated as well (Fig. 2d). It is shown that EE% increased when raising lipid and surfactant concentrations. Similar results were described by Shah et al. (2009), when evaluating EE% of tretinoin in lipid nanoparticles. According to Pokharkar et al. (2011), the probable explanation for the increase of EE% with the increase of lipid concentration is that a higher lipid amount may serve to encapsulate a higher amount of active substance available.

Based on the present results, the NLCs formulation selected to encapsulate carvacrol was the one with the highest lipid and surfactant concentration tested, mainly due to the highest encapsulation efficiency. This NLCs formulation was used to the next experiments.

4.2. Stability of NLCs

The evaluation of NLCs stability is essential to confirm that the structural properties were preserved during the storage time, since structural changes of NLCs as drug delivery systems may impact its therapeutic potential (Zhang et al., 2018).

The stability study of CRV-NLCs formulations stored at room temperature (25 °C) and 4 °C from 24 h until 90 days after the preparation was performed (shown in the supplementary information). In both storage temperatures the particle size stayed almost constant during the period. Large fluctuations in particle size within time could indicate the formation of aggregates, consequently increasing the range of particle size (Zhang et al., 2018). PdI also kept constant, around 0.2, which is a value used to indicate a narrow size distribution. Moreover, the zeta potential of CRV-NLCs formulations varied in the same range, indicating that the particles were kept stable during storage time.

4.3. DSC and XRD characterizations

DSC is an interesting tool to characterize NLCs formulations and its raw materials, providing information about its physical state and crystallinity through thermal behavior (Galvão et al., 2016).

In Fig. 3A is shown the DSC curves of the chosen solid lipid, BW (a), the surfactant P188 (b) and CRV-NLCs. The DSC curve of beeswax presents an endothermic event in the range of 40 to 70 °C (T_{peak} = 64.7 °C) characteristic of its melting point. This result was similar to the event described by our group in previous studies (Dantas et al., 2018; Galvão et al., 2016). The surfactant used in the CRV-NLCs formulation, P188 also showed an endothermic event in the interval of 45 to 65 °C (T_{peak} = 56.32 °C) regarding its melting point (Ige et al., 2013). According to Shah and Serajuddin (2012) (), due to the presence of the poly (ethylene oxide) in the structure, P188 may be used as emulsifying and/or lipid solidification agent, similar to solid PEGs.

The CRV-NLCs exhibited two endothermic peaks in the range of 40 to 70 °C (T_{peak1} = 52.61 °C and T_{peak2} = 63.50). In addition, it was observed that the enthalpy involved in the melting of CRV-NLCs was slightly lowered in comparison to pure bulk BW. This reduction may result from the small particle size of CRV-NLCs and also suggests a disorder of crystalline structure, suggesting that carvacrol is dispersed on lipid matrix (Hu et al., 2006).

XRD is a technique that evaluates how the solid lipid is organized, its phase behavior and crystal ordering. NLCs are composed of solid lipids and modifications in crystallinity may affect its physical stability (Yang et al., 2013; Zheng et al., 2013).

Figure 3B shows the XRD profile of BW, P188, and CRV-NLCs. The beeswax presented three main well-defined diffraction peaks in 2θ: 19.40°, 21.53° and 23.96°, characteristic of its crystalline nature, and P188 presented two main peaks in 2θ: 19.23° e 23.33° (Shah and Serajuddin, 2012; Soleimanian et al., 2018). After CRV-NLCs formation, the intensity of main diffraction peaks was reduced in comparison to the raw materials (BW and P188). According to Tamjidi et al. (2013), this reduction can be attributed to a low ordering of the lipid matrix, resulting in a reduction in crystallinity which confirms the results obtained by DSC analysis.

4.4. Transmission electron microscopy (TEM and cryo-TEM)

Fig. 4a shows the TEM images of CRV-NLCs by using negative staining. It was observed that the particles were of mean particle size close to those found in the particle size analysis by DLS (90 to 150 nm). In addition, the particles had darker edges which may be due to the surfactant P188 layer immobilized in the solid lipid.

Cryo-TEM enabled a direct visualization of the morphology of the obtained particles when dispersed in water. This technique allows the formation of images of complex 3D structures with different orientations. CRV-NLCs possess a typical disk-like morphology, presenting low electron density with a circular shape when viewed from the top; or electron-dense bars when edge-on viewed (white arrows) (Fig. 4b). The discoid structure was previously described for NLCs by Esposito et al., 2017.

4.5. In vitro release experiments

The *in vitro* release profile of carvacrol in solution (CRV-S) and encapsulated (CRV-NLCs) is presented in Fig. 5. Carvacrol was quickly released from CRV-S in comparison to CRV-NLCs, with 100% of cumulative release less than 1 h of starting the experiment. We observed that CRV-NLCs exhibited a biphasic release profile, where a burst release occurred in the first 4 h of experiment (60% of carvacrol), possibly due to the fast diffusion of carvacrol present on the particles surface, followed by an extended release possibly due to diffusion of carvacrol or matrix erosion.

The modeling of active substances release from delivery systems is important for the understanding and the elucidation of the transport mechanisms (Papadopoulou et al., 2006). Therefore, the *in vitro* release data of carvacrol from NLCs were fitted with Korsmeyer and Peppas and Weibull kinetic models. The general expression of Korsmeyer and Peppas is described by the Eq. (4):

$$Mt/M\infty = kt^n \quad (4)$$

where "Mt/M∞" corresponds to the fraction of the active substance released at time t, "k" is the kinetic constant and "n" is the exponent that is related to the diffusion mechanisms involved in the release. Thus, for release systems of sphere type, $n \leq 0.43$ corresponds to Fickian diffusion, $0.85 \leq n \geq 0.43$ corresponds to mixed release mechanism and $n \geq 0.85$ to Case II transport (or non Fickian diffusion) (Tsao and Hall, 2017). In the present study the "n" value found was lower than 0.43 (n = 0,372 e r^2 = 0,950), which corresponds to the Fickian diffusion release mechanism, in other words, the release of carvacrol is driven by the concentration gradient and directly related to its solubility in the NLCs matrix and in the release media. A similar release profile was reported by Kumbhar and Pokharkar (2013) (Kumbhar and Pokharkar, 2013) for bicalutamide, a poorly aqueous soluble drug, from NLCs.

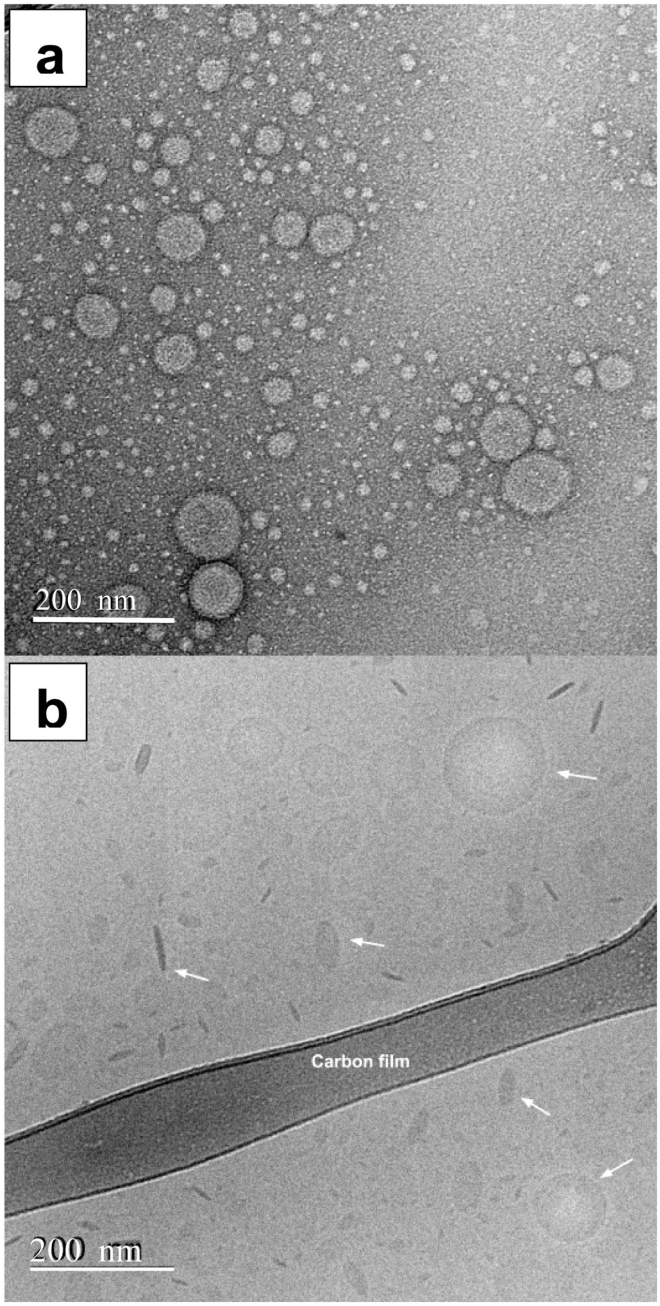

Fig. 4. Photomicrographs of CRV-NLCs obtained by (a) TEM using negative staining, and, (b) Cryotransmission electron microscopy (Cryo-TEM) acquired by using minimum dose system (MDS) in Photo Mode in a transmission electron microscope JEOL JEM-1400Plus. The white arrows show a typical disk-like morphology for CRV-NLCs with low electron density circular shape if viewed from the top, or more electron-dense bars if edge-on viewed. Each panel has scale bar of 200 nm.

The present release profile was also fitted to the Weibull model described by the Eq. (5):

$$Mt/M\infty = 1 - \exp(-at^b) \quad (5)$$

where "Mt/M∞" corresponds to the fraction of the active substance released at a time t, and "a" and "b" constants. The "b" value was

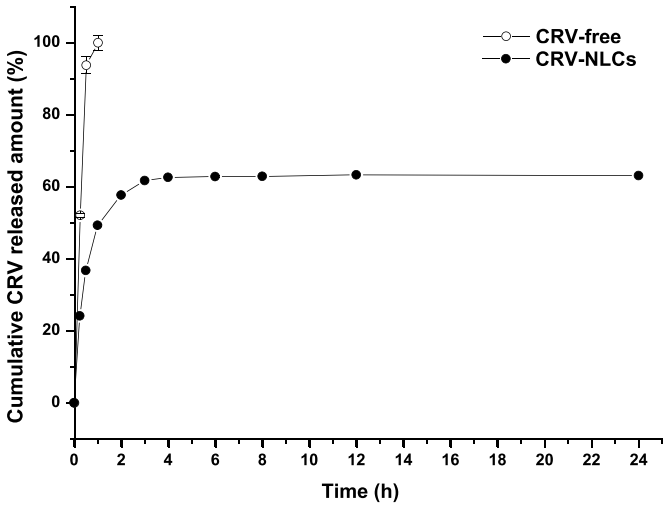

Fig. 5. *In vitro* release profile of carvacrol in solution (CRV-S) and encapsulated in NLCs (CRV-NLC) after 24 h of experiment. Results are representative of three independent experiments. Data are expressed as mean ± SD.

correlated to the diffusion mechanisms involved in the release of active substances by Papadopoulou et al. (2006). The authors correlated "b" value obtained by Weibull equation with "n" value obtained by Korsmeyer and Peppas equation, where $b < 0.75$ corresponds to Fickian diffusion in the Euclidean space ($0.69 < b < 0.75$) or fractal ($b < 0.69$), and $b > 0.75$ corresponds to anomalous transport with more than one release mechanism involved. Therefore, in the present study, the b value found was lower than 0.75 ($b = 0.69$ e $r^2 = 0.9704$) which is related to a Fickian diffusion mechanism, confirming the Korsmeyer e Peppas model results.

4.6. In vitro cytotoxicity in differentiated human monocytic cell line

Considering the promising application of CRV-NLCs in the leishmaniasis treatment, cell viability studies are essential in the development of suitable formulations. The *Leishmania* parasite when in contact with the host, it is phagocytized by macrophages, multiplies and transforms in amastigote forms. Therefore, CRV-NLCs should be capable to being phagocytized by the host cell (macrophage) without causing damage to it.

Table 1 shows the mean cytotoxic concentration for 50% (CC_{50}) for THP-1 cells differentiated in macrophages, after 48 h of treatment using CRV-S, CRV-NLCs and miltefosine (conventional anti-leishmania drug). It is possible to observe that CRV-S and CRV-NLCs presented much lower cytotoxicity to THP-1 differentiated cells in comparison to the conventional leishmanicidal drug, miltefosine (MT) ($p < 0.005$). After the encapsulation in NLCs, carvacrol showed lower cytotoxicity in comparison to CRV-S ($p < 0.05$). This result suggests the protective role of NLCs formulations to mammalian cells. Lopes et al. (2012) also reported a decrease in the cytotoxicity of THP-1 differentiated cells after the encapsulation of the drug oryzalin in solid lipid nanoparticles using tripalmitin as solid lipid.

Table 1
Mean inhibitory concentration (IC_{50}) for 50% of L. *amazonensis* promastigotes and mean cytotoxic concentration for 50% of differentiated THP1 cells (CC_{50}) after 48 h of incubation with different concentrations of carvacrol in solution (CRV-S) or encapsulated (CRV-NLCs) and miltefosine (MT) (used as positive control). Results are representative of three independent experiments. Data are expressed as mean ± SD. $n = 3$, ns, no significant statistical difference, $^*p < 0.05$, significant statistical difference in comparison to CRV in solution (CRV-S) (Student`s *t*-test).

Samples	L. *amazonensis* promastigotes IC_{50} (μg/mL)	Differentiated THP1 cellsCC_{50} (μg/mL)
CRV-S	28.1 ± 0.3	64.1 ± 1.6
CRV-NLCs	28.2 ± 3.25ns	73.5 ± 1.6*
MT	17.12 ± 1.3	12.8 ± 0.7

4.7. In vitro leishmanicidal activity

The mean inhibitory concentration for 50% (IC_{50}) of L. *amazonensis* promastigotes treated with CRV-S, CRV-NLCs and miltefosine is shown in Table 1. Miltefosine was tested as positive control, since this drug is used in the leishmaniasis conventional treatment. Carvacrol in the present study showed an IC_{50} of 28.1 ± 0.3 μg/mL, being close to the IC_{50} observed by Silva et al. (2017), 25.4 ± 2.4 μg/mL, for the same *Leishmania* species. Youssefi et al. (2019) reported a lower IC_{50} when the carvacrol was tested against other species, *leishmania infantum* (9.8 μg/mL). As observed in Table 1, CRV-NLCs presented IC_{50} close to CRV-S. This is probably due to the presence of CRV in NLCs surface (~ 60%), which was quickly released according to the *in vitro* release profile shown previously. Therefore, it is suggested that the actual CRV-NLCs activity would be even higher than CRV-S considering that part of CRV is still confined in NLCs (~ 40%), and not in direct contact with the parasite. Other studies in the literature have also reported unchanged activity over promastigotes after encapsulation. Moreno et al. (2015) reported that the β-lapachone encapsulated in chitosan-lecithin nanoparticles maintained the same level of activity over L. *major* promastigotes compared to free β-lapachone. Van de Ven et al. (2011) also observed that the saponin β-aescin encapsulated in PLGA nanoparticles showed the same efficacy against L. *infantum* promastigotes in comparison to free β-aescin.

4.8. Antiamastigote activity

In Table 2, it is presented the mean inhibitory concentration for 50% (IC_{50}) of L. *amazonensis* amastigotes treated with CRV-S, CRV-NLCs and amphothericin B (used as positive control). The antileishmanial activity of CRV-S in the amastigote form compared with the promastigote form did not change significantly (IC_{50} = 28.1 and IC_{50} = 27.40). Moreover, CRV loaded in NLCs showed higher activity in the amastigote form (IC_{50} = 19.65) than in promastigote form (IC_{50} = 28.2). According to Moreno et al., 2015, this may suggest a possible immunomodulatory effect for the system. In addition, CRV-NLCs showed less toxicity to peritoneal macrophages than CRV-S and consequently increasing the selectivity index (SI) of carvacrol.

4.9. In vivo pharmacokinetics study

Fig. 6 shows the *in vivo* pharmacokinetic profile of carvacrol in solution (CRV-S) and encapsulated (CRV-NLCs) in Wistar rats after I.V. bolus administration (3 mg/kg). We observed that CRV, in the administered dose, suggests that this phenolic monoterpene probably undergo enterohepatic recirculation, since it is possible to observe initially (two first hours) a decrease in plasma concentration followed by an increase in concentration and a decrease again, which is called "zigue zague" profile. In the enterohepatic recirculation, the active substance arrives in the systemic circulation, passing through the liver, being metabolized and its metabolites are excreted with bile, by the gall bladder in the duodenum. In the gut, its metabolites are converted to the original active substance by the gut flora and soon after being reabsorbed by portal circulation. Therefore, some fraction of the active substance present in the gut may be reabsorbed and returns to the liver where the enterohepatic recirculation repeats (Roberts et al., 2002).

Several drugs have been reported to undergo enterohepatic circulation such as warfarin, morphine, erythromycin, doxycycline, ceftriaxone, and others. A recent review identified more than 45 drugs that undergo enterohepatic circulation (Gao et al., 2014). In general, drugs or active substances that undergo enterohepatic circulation are small

Table 2
Mean inhibitory concentration (IC_{50}) for 50% of L. *amazonensis* amastigotes and mean cytotoxic concentration for 50% of peritoneal macrophages (CC_{50}) after 72 h of incubation with different concentrations of carvacrol in solution (CRV-S) or encapsulated (CRV-NLCs) and amphotericin B (used as positive control). Results are representative of three independent experiments. Data are expressed as mean ± SD. $n = 3$, ns, no significant statistical difference, $^{*}p < 0.05$, significant statistical difference in comparison to CRV in solution (CRV-S) (Student`s *t*-test).

Samples	L. *amazonensis* amastigotes(μg/mL)	CC_{50} (μg/mL)(Peritoneal macrophages)	SI(Peritoneal macrophages)	CC_{50} (μg/mL)(THP1)	SI(THP1)
CRV-S	27.40 ± 2.05	35.27 ± 5.79	1.28	64.1	2.3
CRV-NLCs	19.65 ± 1.3**	49.05 ± 2.04***	2.50	73.5	3.74
Amphotericin B	0.27 ± 0.05	>20	–	–	–

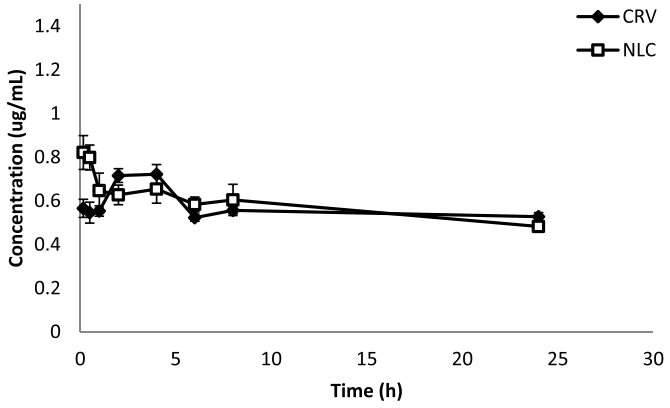

Fig. 6. *In vivo* pharmacokinetic profile after intravenous administration in bolus (3 mg/kg) of carvacrol in solution (CRV-S) and encapsulated (CRV-NLCs) in Wistar rats. Results are representative of three independent experiments. Data are expressed as mean ± SD.

nonpolar molecules as carvacrol (Okour and Brundage, 2017). Other phenolic compounds have been reported to present pharmacokinetic profile similar to carvacrol, such as, the ginger derivatives, 6-gingerol (6 G), 8-gingerol (8 G), 10-gingerol (10 G) e 6-shogaol (6S) (Mukkavilli et al., 2017).

Plasma concentration-time profile was submitted to non-compartmental analysis (Table 3). CRV presented elimination half-life ($t_{1/2}$) of 51.07 ± 2.80 h, clearance (CL) of 0.057 ± 0,003 L/h and initial plasma concentration (C_0) of 0.59 ± 0.075 μg/mL. These results are in agreement with expectations for compounds that undergo enterohepatic circulation since the gut reabsorption tends to promote a long elimination half-life and low clearance value. There are no reports in the literature about the enterohepatic circulation of carvacrol. This is probably because the dose used on the past studies was much lower than the dose administered in the present study, and/or the difference in the administration route used was extravascular (oral, topical and intramammary).

Table 3
Pharmacokinetic data obtained from the non-compartmental analysis of *in vivo* pharmacokinetic profile after intravenous administration of carvacrol in solution (CRV-S) and encapsulated (CRV-NLCs) in Wistar rats. Results are representative of three independent experiments. Data are expressed as mean ± SD. $n = 3$, ns, no significant statistical difference, $^{*}p < 0.05$ and $^{**}p < 0.01$, significant statistical difference in comparison to CRV in solution (CRV-S) (Student`s *t*-test).

Pharmacokinetic parameters	CRV-S	CRV-NLCs	p-value
t ½ (h)	51.07 ± 2.80	69.33 ± 7.30*	0.0150
C_0 (μg/mL)	0.59 ± 0.075	0.89 ± 0.14*	0.027
CL (L/h)	0.057 ± 0.003	0.048 ± 0.005	Ns
V_{dss} (L)	4.37 ± 0.079	4.83 ± 0.12**	0.0052
AUC_{total} (μg h/L)	13.62 ± 0.311	13.38 ± 0.57	Ns
MRT (h)	75.29 ± 4.09	99.67 ± 9.99*	0.0166

The pharmacokinetic profile of carvacrol in solution (CRV-S) was similar to the encapsulated (CRV-NLCs). However, after non-compartmental analysis, we observed that C_0, $t_{1/2}$ and mean residence time (MRT) of CRV-NLCs was higher than CRV-S ($p < 0.05$). Moreover, the volume of distribution (V_{dss}) of CRV-NLCs was higher than CRV-S ($p < 0.01$). This increase in V_{dss} probably occurred due to the lipid nature of NLCs that favored a higher distribution of carvacrol in tissues, consequently resulting in a higher C_0, $t_{1/2}$ and mean residence time (MRT) than CRV-S. In the literature, drugs and active substances encapsulated in NLCs have been reported to increase the $t_{1/2}$ and MRT (Shi et al., 2016; Singh et al., 2016). According to Tsai et al. (2012), the active compound can be protected from metabolism and excretion when it is carried in NLCs.

However, as the pharmacokinetic profile showed that CRV undergo enterohepatic circulation and consequently providing a long $t_{1/2}$ and higher circulation time, it is expected that after the encapsulation in NLCs the profile did not change much from the CRV-S that explains why the area under the curve total (AUC_{total}) did not change significantly after carvacrol encapsulation in NLCs (ns). Although the CRV-NLCs showed similar exposure (AUC_{total}) to CRV-S, the higher MRT and V_{dss} of encapsulated carvacrol would favor a higher distribution of carvacrol in the target organs, such as liver and spleen, where *Leishmania* resides.

5. Conclusion

Using a warm microemulsion method CRV-NLCs were optimized with beeswax (HLB = 9) as the solid lipid and the combination of 5% of lipids and surfactant. The selected CRV-NLCs formulation shows particle size, PDI and zeta potential suitable for parenteral administration. High encapsulation efficiency of CRV in NLCs formulation was achieved. Preliminary stability studies showed that CRV-NLCs were stable during the storage time of 90 days. Furthermore, the crystal order of beeswax was disturbed in the inner cores of CRV-NLCs according to DSC and XRD profiles.

The *in vitro* release of carvacrol from NLCs demonstrated that the release mechanism is probably by Fickian diffusion. Moreover, carvacrol encapsulation in NLCs provided lower cytotoxicity in comparison to free carvacrol and increased its *in vitro* leishmanicidal efficacy in the amastigote form, improving the selectivity index of CRV. Finally, the *in vivo* pharmacokinetics of carvacrol after IV bolus administration suggests that this phenolic monoterpene undergoes enterohepatic circulation and therefore shows a long half-life ($t_{1/2}$) and low value of clearance (CL). In addition, C_0, mean residence time (MRT) and V_{dss} of encapsulated carvacrol were higher than free carvacrol favoring a higher distribution of carvacrol in the target tissues (liver and spleen). Thus, CRV-NLCs are a promising formulation for leishmaniasis treatment, and may be in future this formulation may serve as a platform for surface modifications for the binding of ligands with affinity for macrophage receptors, aiming to further increase the selectivity of carvacrol for the *Leishmania* parasite. Moreover, the next step in the development of drug delivery system to treat leishmaniasis would be the *in vivo* efficacy assays in mice.

CRediT authorship contribution statement

Juliana G. Galvão: Conceptualization, Investigation, Methodology, Formal analysis, Writing - original draft, Writing - review & editing. **Raquel L. Santos:** Investigation. **Audrey R.S.T. Silva:** Investigation. **Jeferson S. Santos:** Investigation. **Amanda M.B. Costa:** Investigation. **Hardik Chandasana:** Methodology, Investigation, Formal analysis. **Valter V. Andrade-Neto:** Methodology, Investigation, Formal analysis. **Eduardo Caio Torres-Santos:** Methodology, Investigation, Formal analysis. **Ana Amélia M. Lira:** Supervision. **Silvio Dolabella:** Supervision. **Ricardo Scher:** Methodology, Resources, Supervision, Writing - review & editing. **Peter E. Kima:** Methodology, Resources, Writing - review & editing. **Hartmut Derendorf:** Methodology, Resources, Supervision, Writing - review & editing. **Rogéria S. Nunes:** Supervision, Conceptualization, Project administration, Funding acquisition, Visualization, Resources.

Acknowledgements

We gratefully acknowledge the Conselho Nacional de Desenvolvimento Científico e Tecnológico (CNPq/Brazil) for supporting funds, and the Coordenação de Aperfeiçoamento de Pessoal de Nível Superior (CAPES/Brazil) that financed in part this study – Finance Code 001. We also acknowledge the Electron Microscopy Laboratory (LME) at the Brazilian Nanotechnology National Laboratory (LNNano), CNPEM, Campinas, Brazil for their support with the TEM and Cryo-TEM analysis. Juliana G. Galvão is grateful for the Doctoral Dissertation Research Award granted by Fulbright Commission (USA-Brazil).

Supplementary materials

Supplementary material associated with this article can be found, in the online version, at doi:10.1016/j.ejps.2020.105335.

References

Arunasree, K.M., 2010. Anti-proliferative effects of carvacrol on a human metastatic breast cancer cell line, MDA-MB 231. Phytomedicine 17, 581–588. https://doi.org/10.1016/j.phymed.2009.12.008.

Beena, Kumar, D., Rawat, D.S., 2013. Synthesis and antioxidant activity of thymol and carvacrol based Schiff bases. Bioorg. Med. Chem. Lett. https://doi.org/10.1016/j.bmcl.2012.12.001.

Belda-Galbis, C.M., Leufvén, A., Martínez, A., Rodrigo, D., 2014. Predictive microbiology quantification of the antimicrobial effect of carvacrol. J. Food Eng. 141, 37–43. https://doi.org/10.1016/j.jfoodeng.2014.05.013.

Bruni, N., Stella, B., Giraudo, L., Della Pepa, C., Gastaldi, D., Dosio, F., 2017. Nanostructured delivery systems with improved leishmanicidal activity: a critical review. Int. J. Nanomed. 12, 5289–5311. https://doi.org/10.2147/IJN.S140363.

Dantas, I.L., Bastos, K.T.S., Machado, M., Galvão, J.G., Lima, A.D., Gonsalves, J.K.M.C., Almeida, E.D.P., Araújo, A.A.S., de Meneses, C.T., Sarmento, V.H.V., Nunes, R.S., Lira, A.A.M., 2018. Influence of stearic acid and beeswax as solid lipid matrix of lipid nanoparticles containing tacrolimus. J. Therm. Anal. Calorim. https://doi.org/10.1007/s10973-018-7072-7.

De Almeida, L., Fujimura, A.T., Del Cistia, M.L., Fonseca-Santos, B., Imamura, K.B., Michels, P.A.M., Chorilli, M., Graminha, M.A.S., 2017. Nanotechnological strategies for treatment of leishmaniasis-a review. J. Biomed. Nanotechnol. 13, 117–133. https://doi.org/10.1166/jbn.2017.2349.

de Medeiros, M., das, G.F., da Silva, A.C., Citó, A.M., das, G.L., Borges, A.R., de Lima, S.G., Lopes, J.A.D., Figueiredo, R.C.B.Q., 2011. *In vitro* antileishmanial activity and cytotoxicity of essential oil from Lippia sidoides Cham. Parasitol. Int. 60, 237–241. https://doi.org/10.1016/j.parint.2011.03.004.

de Melo, J.O., Bitencourt, T.A., Fachin, A.L., Cruz, E.M.O., de Jesus, H.C.R., Alves, P.B., de Fátima Arrigoni-Blank, M., de Castro Franca, S., Beleboni, R.O., Fernandes, R.P.M., Blank, A.F., Scher, R., 2013. Antidermatophytic and antileishmanial activities of essential oils from Lippia gracilis Schauer genotypes. Acta Trop. 128, 110–115. https://doi.org/10.1016/j.actatropica.2013.06.024.

de Sousa, D.P., 2011. Analgesic-like activity of essential oils constituents. Molecules 16, 2233–2252. https://doi.org/10.3390/molecules16032233.

de Souza, A., Marins, D.S.S., Mathias, S.L., Monteiro, L.M., Yukuyama, M.N., Scarim, C.B., Löbenberg, R., Bou-Chacra, N.A., 2018. Promising nanotherapy in treating leishmaniasis. Int. J. Pharm. 547, 421–431. https://doi.org/10.1016/j.ijpharm.2018.06.018.

Esposito, E., Drechsler, M., Mariani, P., Carducci, F., Servadio, M., Melancia, F., Ratano, P., Campolongo, P., Trezza, V., Cortesi, R., Nastruzzi, C., 2017. Lipid nanoparticles for administration of poorly water soluble neuroactive drugs. Biomed. Microdevices. https://doi.org/10.1007/s10544-017-0188-x.

Fangueiro, J.F., Calpena, A.C., Clares, B., Andreani, T., Egea, M.A., Veiga, F.J., Garcia, M.L., Silva, A.M., Souto, E.B., 2016. Biopharmaceutical evaluation of epigallocatechin gallate-loaded cationic lipid nanoparticles (EGCG-LNs): *in vivo, in vitro* and ex vivo studies. Int. J. Pharm. 502, 161–169. https://doi.org/10.1016/j.ijpharm.2016.02.039.

Galvão, J.G., Trindade, G.G.G., Santos, A.J., Santos, R.L., Chaves Filho, A.B., Lira, A.A.M., Miyamoto, S., Nunes, R.S., 2016. Effect of Ouratea sp. butter in the crystallinity of solid lipids used in nanostructured lipid carriers (NLCs). J. Therm. Anal. Calorim 123, 941–948. https://doi.org/10.1007/s10973-015-4890-8.

Gao, Y., Shao, J., Jiang, Z., Chen, J., Gu, S., Yu, S., Zheng, K., Jia, L., 2014. Drug enterohepatic circulation and disposition: constituents of systems pharmacokinetics. Drug Discov. Today 19, 326–340. https://doi.org/10.1016/j.drudis.2013.11.020.

Guterres, S.S., Alves, M.P., Pohlmann, A.R., 2007. Polymeric nanoparticles, nanospheres and nanocapsules, for cutaneous applications. Drug Target Insights 2, 147–157.

Han, F., Li, S., Yin, R., Liu, H., Xu, L., 2008. Effect of surfactants on the formation and characterization of a new type of colloidal drug delivery system: nanostructured lipid carriers. Colloids Surfaces A Physicochem. Eng. Asp. 315, 210–216. https://doi.org/10.1016/j.colsurfa.2007.08.005.

Hu, F.Q., Jiang, S.P., Du, Y.Z., Yuan, H., Ye, Y.Q., Zeng, S., 2006. Preparation and characteristics of monostearin nanostructured lipid carriers. Int. J. Pharm. 314, 83–89. https://doi.org/10.1016/j.ijpharm.2006.01.040.

Ige, P.P., Baria, R.K., Gattani, S.G., 2013. Fabrication of fenofibrate nanocrystals by probe sonication method for enhancement of dissolution rate and oral bioavailability. Colloids Surfaces B Biointerfaces 108, 366–373. https://doi.org/10.1016/j.colsurfb.2013.02.043.

Kumbhar, D.D., Pokharkar, V.B., 2013. Engineering of a nanostructured lipid carrier for the poorly water-soluble drug, bicalutamide: physicochemical investigations. Colloids Surfaces A Physicochem. Eng. Asp. 416, 32–42. https://doi.org/10.1016/J.COLSURFA.2012.10.031.

Lakshmi, P., Kumar, G.A., 2010. Review artice nano suspension TECHNOLOGY : a review. Int. J. Pharm. Pharm. Sci. 2, 35–40.

Lopes, R., Eleutério, C.V., Gonalves, L.M.D., Cruz, M.E.M., Almeida, A.J., 2012. Lipid nanoparticles containing oryzalin for the treatment of leishmaniasis. Eur. J. Pharm. Sci. 45, 442–450. https://doi.org/10.1016/j.ejps.2011.09.017.

Mehnert, W., Mäder, K., 2012. Solid lipid nanoparticles: production, characterization and applications. Adv. Drug Deliv. Rev. 64, 83–101. https://doi.org/10.1016/j.addr.2012.09.021.

Ministério da saúde, 2017. Casos de leishmaniose tegumentar. brasil, grandes regiões e unidades federadas. 1990 a 2016.

Mitri, K., Shegokar, R., Gohla, S., Anselmi, C., Müller, R.H., 2011. Lipid nanocarriers for dermal delivery of lutein: preparation, characterization, stability and performance. Int. J. Pharm. 414, 267–275. https://doi.org/10.1016/j.ijpharm.2011.05.008.

Monzote, L., García, M., Pastor, J., Gil, L., Scull, R., Maes, L., Cos, P., Gille, L., 2014. Essential oil from chenopodium ambrosioides and main components: activity against Leishmania, their mitochondria and other microorganisms. Exp. Parasitol. 136, 20–26. https://doi.org/10.1016/j.exppara.2013.10.007.

Monzote, L., Pastor, J., Scull, R., Gille, L., 2014. Antileishmanial activity of essential oil from Chenopodium ambrosioides and its main components against experimental cutaneous leishmaniasis in BALB/c mice. Phytomedicine 21, 1048–1052. https://doi.org/10.1016/j.phymed.2014.03.002.

Moreno, E., Schwartz, J., Larrea, E., Conde, I., Font, M., Sanmartín, C., Irache, J.M., Espuelas, S., 2015. Assessment of β-lapachone loaded in lecithin-chitosan nanoparticles for the topical treatment of cutaneous leishmaniasis in L. major infected BALB/c mice. Nanomed. Nanotechnol. Biol. Med. 11, 2003–2012. https://doi.org/10.1016/j.nano.2015.07.011.

Mukkavilli, R., Yang, C., Tanwar, R.S., Ghareeb, A., Luthra, L., Aneja, R., 2017. Absorption, metabolic stability, & pharmacokinetics of ginger phytochemicals. Molecules 22. https://doi.org/10.3390/molecules22040553.

Müller, R.H., Mäder, K., Gohla, S., 2000. Solid lipid nanoparticles (SLN) for controlled drug delivery - a review of the state of the art. Eur. J. Pharm. Biopharm. 50, 161–177.

Müller, R.H., Petersen, R.D., Hommoss, A., Pardeike, J., 2007. Nanostructured lipid carriers (NLC) in cosmetic dermal products. Adv. Drug Deliv. Rev. 59, 522–530. https://doi.org/10.1016/j.addr.2007.04.012.

Müller, R.H., Radtke, M., Wissing, S.A., 2002. Nanostructured lipid matrices for improved microencapsulation of drugs. Int. J. Pharm. 242, 121–128. https://doi.org/10.1016/S0378-5173(02)00180-1.

Okour, M., Brundage, R.C., 2017. Modeling enterohepatic circulation. Curr. Pharmacol. Rep. 3, 301–313. https://doi.org/10.1007/s40495-017-0096-z.

Organization, W.H., 2016. Leishmaniasis in high-burden countries: an epidemiological update based on data reported in 2014.

Papadopoulou, V., Kosmidis, K., Vlachou, M., Macheras, P., 2006. On the use of the Weibull function for the discernment of drug release mechanisms. Int. J. Pharm. 309, 44–50. https://doi.org/10.1016/J.IJPHARM.2005.10.044.

Pastor, J., García, M., Steinbauer, S., Setzer, W.N., Scull, R., Gille, L., Monzote, L., 2015. Combinations of ascaridole, carvacrol, and caryophyllene oxide against leishmania. Acta Trop 145, 31–38. https://doi.org/10.1016/j.actatropica.2015.02.002.

Pham, T.T.H., Barratt, G., Michel, J.P., Loiseau, P.M., Saint-Pierre-Chazalet, M., 2013. Interactions of antileishmanial drugs with monolayers of lipids used in the development of amphotericin B-miltefosine-loaded nanocochleates. Colloids Surfaces B Biointerfaces 106, 224–233. https://doi.org/10.1016/j.colsurfb.2013.01.041.

Pham, T.T.H., Gueutin, C., Cheron, M., Abreu, S., Chaminade, P., Loiseau, P.M., Barratt, G., 2014. Development of antileishmanial lipid nanocomplexes. Biochimie 107, 143–153. https://doi.org/10.1016/j.biochi.2014.06.007.

Pokharkar, V.B., Shekhawat, P.B., Dhapte, V.V., Mandpe, L.P., 2011. DEVELOPMENT and optimization of eugenol loaded nanostructured lipid carriers for periodontal delivery. Int. J. Pharm. Pharm. Sci. 3, 138–143.

Polonio, T., Efferth, T., 2008. Leishmaniasis: drug resistance and natural products (review). Int. J. Mol. Med. 22, 277–286.
Ribeiro, L.N.M., Franz-Montan, M., Breitkreitz, M.C., Alcântara, A.C.S., Castro, S.R., Guilherme, V.A., Barbosa, R.M., de Paula, E., 2016. Nanostructured lipid carriers as robust systems for topical lidocaine-prilocaine release in dentistry. Eur. J. Pharm. Sci. 93, 192–202. https://doi.org/10.1016/j.ejps.2016.08.030.
Roberts, M.S., Magnusson, B.M., Burczynski, F.J., Weiss, M., 2002. Enterohepatic circulation: physiological, pharmacokinetic and clinical implications. Clin. Pharmacokinet. 41, 751–790. https://doi.org/10.2165/00003088-200241100-00005.
Santos, E.H., Kamimura, J.A., Hill, L.E., Gomes, C.L., 2015. Characterization of carvacrol beta-cyclodextrin inclusion complexes as delivery systems for antibacterial and antioxidant applications. LWT - Food Sci. Technol. 60, 583–592. https://doi.org/10.1016/j.lwt.2014.08.046.
Saúde, M.da, 2017. Casos confirmados de leishmaniose visceral, brasil, grandes regiões e unidades federadas. 1990 a 2016.
Schubert, M.A., Müller-Goymann, C.C., 2003. Solvent injection as a new approach for manufacturing lipid nanoparticles–evaluation of the method and process parameters. Eur. J. Pharm. Biopharm. 55, 125–131.
Shah, K.A., Joshi, M.D., Patravale, V.B., 2009. Biocompatible microemulsions for fabrication of glyceryl monostearate solid lipid nanoparticles (SLN) of tretinoin. J. Biomed. Nanotechnol. 5, 396–400.
Shah, A.V., Serajuddin, A.T.M., 2012. Development of solid self-emulsifying drug delivery system (SEDDS) I: use of poloxamer 188 as both solidifying and emulsifying agent for lipids. Pharm. Res. 29, 2817–2832. https://doi.org/10.1007/s11095-012-0704-x.
Shi, F., Zhao, Y., Firempong, C.K., Xu, X., 2016. Preparation, characterization and pharmacokinetic studies of linalool-loaded nanostructured lipid carriers. Pharm. Biol. 54, 2320–2328. https://doi.org/10.3109/13880209.2016.1155630.
Silva, A.R.S.T., Scher, R., Santos, F.V., Ferreira, S.R., Cavalcanti, S.C.H., Correa, C.B., Bueno, L.L., Alves, R.J., Souza, D.P., Fujiwara, R.T., Dolabella, S.S., 2017. Leishmanicidal activity and structure-activity relationships of essential oil constituents. Molecules 22. https://doi.org/10.3390/molecules22050815.
Silva, F.V., Guimarães, A.G., Silva, E.R.S., Sousa-Neto, B.P., Machado, F.D.F., Quintans-Júnior, L.J., Arcanjo, D.D.R., Oliveira, F.A., Oliveira, R.C.M., 2012. Anti-Inflammatory and anti-ulcer activities of carvacrol, a monoterpene present in the essential oil of oregano. J. Med. Food 15, 984–991. https://doi.org/10.1089/jmf.2012.0102.
Singh, I., Swami, R., Pooja, D., Jeengar, M.K., Khan, W., Sistla, R., 2016. Lactoferrin bioconjugated solid lipid nanoparticles: a new drug delivery system for potential brain targeting. J. Drug Target. 24, 212–223. https://doi.org/10.3109/1061186X.2015.1068320.
Sizílio, R.H., Galvão, J.G., Trindade, G.G.G., Pina, L.T.S., Andrade, L.N., Gonsalves, J.K.M.C., Lira, A.A.M., Chaud, M.V., Alves, T.F.R., Arguelho, M.L.P.M., Nunes, R.S., 2018. Chitosan/pvp-based mucoadhesive membranes as a promising delivery system of betamethasone-17-valerate for aphthous stomatitis. Carbohydr. Polym. 190. https://doi.org/10.1016/j.carbpol.2018.02.079.
Soleimanian, Y., Goli, S.A.H., Varshosaz, J., Sahafi, S.M., 2018. Formulation and characterization of novel nanostructured lipid carriers made from beeswax, propolis wax and pomegranate seed oil. Food Chem 244, 83–92. https://doi.org/10.1016/J.FOODCHEM.2017.10.010.
Tamjidi, F., Shahedi, M., Varshosaz, J., Nasirpour, A., 2013. Nanostructured lipid carriers (NLC): a potential delivery system for bioactive food molecules. Innov. Food Sci. Emerg. Technol. 19, 29–43. https://doi.org/10.1016/j.ifset.2013.03.002.
Teeranachaideekul, V., Chantaburanan, T., Junyaprasert, V.B., 2017. Influence of state and crystallinity of lipid matrix on physicochemical properties and permeation of capsaicin-loaded lipid nanoparticles for topical delivery. J. Drug Deliv. Sci. Technol. 39, 300–307. https://doi.org/10.1016/J.JDDST.2017.04.003.
Tiuman, T.S., Santos, A.O., Ueda-Nakamura, T., Filho, B.P.D., Nakamura, C.V., 2011. Recent advances in leishmaniasis treatment. Int. J. Infect. Dis. 15. https://doi.org/10.1016/j.ijid.2011.03.021.
Tsai, M.-J., Wu, P.-C., Huang, Y.-B., Chang, J.-S., Lin, C.-L., Tsai, Y.-H., Fang, J.-Y., 2012. Baicalein loaded in tocol nanostructured lipid carriers (tocol NLCs) for enhanced stability and brain targeting. Int. J. Pharm. 423, 461–470. https://doi.org/10.1016/j.ijpharm.2011.12.009.
Tsao, N.H., Hall, E.A.H., 2017. Model for microcapsule drug release with ultrasound-activated enhancement. Langmuir 33, 12960–12972. https://doi.org/10.1021/acs.langmuir.7b02954.
World Health Organization (WHO). 2018. Leishmaniasis [WWW document]. URL https://www.who.int/en/news-room/fact-sheets/detail/leishmaniasis (accessed 12.11.18).
Yan, F., Zhang, C., Zheng, Y., Mei, L., Tang, L., Song, C., Sun, H., Huang, L., 2010. The effect of poloxamer 188 on nanoparticle morphology, size, cancer cell uptake, and cytotoxicity. Nanomed. Nanotechnol. Biol. Med. 6, 170–178. https://doi.org/10.1016/j.nano.2009.05.004.
Yang, X., Zhao, L., Almasy, L., Garamus, V.M., Zou, A., Willumeit, R., Fan, S., 2013. Preparation and characterization of 4-dedimethylamino sancycline (CMT-3) loaded nanostructured lipid carrier (CMT-3/NLC) formulations. Int. J. Pharm. 450, 225–234. https://doi.org/10.1016/j.ijpharm.2013.04.021.
Youssefi, M.R., Moghaddas, E., Tabari, M.A., Moghadamnia, A.A., Hosseini, S.M., Hosseini Farash, B.R., Ebrahimi, M.A., Mousavi, N.N., Fata, A., Maggi, F., Petrelli, R., Dall'Acqua, S., Benelli, G., Sut, S., 2019. In vitro and in vivo effectiveness of carvacrol, thymol and linalool against leishmania infantum. Molecules 24, 1–11. https://doi.org/10.3390/molecules24112072.
Zhang, J., Xiao, X., Zhu, J., Gao, Z., Lai, X., Zhu, X., Mao, G., 2018. Lactoferrin- and RGD-comodified, temozolomide and vincristine-coloaded nanostructured lipid carriers for gliomatosis cerebri combination therapy. Int. J. Nanomed. Volume 13, 3039–3051. https://doi.org/10.2147/IJN.S161163.
Zheng, K., Zou, A., Yang, X., Liu, F., Xia, Q., Ye, R., Mu, B., 2013. The effect of polymer-surfactant emulsifying agent on the formation and stability of α-lipoic acid loaded nanostructured lipid carriers (NLC). Food Hydrocoll. 32, 72–78. https://doi.org/10.1016/j.foodhyd.2012.11.006.